

# Lowering the Percolation Threshold of Conductive Composites Using Particulate Polymer Microstructure

JAIME C. GRUNLAN, WILLIAM W. GERBERICH, LORRAINE F. FRANCIS

Department of Chemical Engineering and Materials Science, University of Minnesota, Minneapolis, Minnesota 55455

Received 28 January 2000; accepted 27 July 2000

**ABSTRACT:** The percolation thresholds of carbon black–polymer composites have been successfully lowered using particulate polymer starting materials (i.e., latex and water-dispersible powder). Composites prepared using carbon black (CB) and commercial poly(vinyl acetate) (PVAc) latex exhibit a percolation threshold near 2.5 vol % CB. This threshold value is significantly lower than that of a comparable reference composite made from poly(*N*-vinylpyrrolidone) (PNVP) solution and the same CB, which exhibits a sharp rise in electrical conductivity near 15 vol % CB. This dramatic difference in critical CB concentration results from the segregated microstructure induced by the latex during composite film formation. Carbon black particles are forced into conductive pathways at low concentration because of their inability to occupy volume already claimed by the much larger latex particles. There appears to be good qualitative agreement between experimental findings and current models dealing with conductive behavior of composites with segregated microstructures. Lack of quantitative agreement with the models is attributed to the polydispersity of the polymer particles in the latex. © 2001 John Wiley & Sons, Inc. *J Appl Polym Sci* 80: 692–705, 2001

**Key words:** percolation threshold; carbon black; latex; polymer composite; electrically conductive

## INTRODUCTION

During the past few decades, electrically conductive polymer composites have found use in a variety of applications. Binary composite systems, comprised of conductive filler (e.g., carbon black, metal powder, etc.) in a polymer matrix, create a material that is tough, flexible, and electrically conductive. These unique materials are ideally suited for antistatic layers,<sup>1,2</sup> electromagnetic interference shielding,<sup>3</sup> chemical vapor sensors,<sup>4–7</sup> and thermal resistors.<sup>8</sup> Despite a growing number of potential applications, these composites are plagued by a serious drawback. The amount of

conductive filler required to achieve a sufficient level of electrical conductivity often leads to processing difficulties and brittle films.<sup>9,10</sup> Lowering the percolation threshold of a composite system appears to be an effective way to reduce the amount of filler required to produce adequate conductivity and thereby minimize problems with mechanical performance.

Percolation can be defined as a phase-transition at which a dramatic change occurs at one sharply defined parametric value, as this parameter is continuously changed.<sup>11</sup> In the case of polymer composites filled with carbon black, the electrical conductivity changes by many orders of magnitude at a precise volume fraction of filler. The concentration of carbon black that marks this insulator–conductor transition is often referred to as the percolation threshold. This sudden jump

---

Correspondence to: L. Francis (lfrancis@tc.umin.edu).

*Journal of Applied Polymer Science*, Vol. 80, 692–705 (2001)  
© 2001 John Wiley & Sons, Inc.

in conductivity is attributed to the formation of the first “infinite” agglomerate pathway that allows electrons to travel a macroscopic distance through the composite.<sup>12,13</sup> Many simple binary composites have a percolation threshold around 15 vol % filler,<sup>14–16</sup> as would be predicted by classical percolation theory for a random system.<sup>17</sup> Random resistor networks, such as filled polymers, typically obey a power-law conductivity relationship after the percolation threshold of the form:

$$\sigma = \sigma_0(V - V_c)^s \quad (1)$$

where  $\sigma$  is the composite conductivity (S/cm),  $\sigma_0$  is the intrinsic conductivity of the filler,  $s$  is the power-law exponent (typically 1.6–2.0 in 3D), and  $V_c$  is the volume fraction of filler at the percolation threshold (near 0.15 for random 3D systems).<sup>18</sup> At concentrations well above the percolation threshold, the rise in conductivity with further addition of filler departs from the behavior described by Eq. 2 and becomes much more gradual as a result of the lack of new conductive pathway formation.<sup>19</sup> Many approaches are now being explored to reduce the percolation threshold, thereby achieving near-maximum conductivity at much lower concentrations of conductive filler.

Percolation thresholds have already been successfully reduced using ternary composite systems in which carbon black has been incorporated into a mixture of two immiscible polymers.<sup>10,20–22</sup> Sumita and coworkers<sup>20</sup> were the first to exploit the use of matrix blends and were able to significantly reduce the percolation threshold. Carbon black was found to aggregate at the interface of the two polymers, which led to more efficient formation of conductive pathways. The surface energies of the two polymers seem to determine where the carbon black will localize. The critical volume fraction ( $V_c$ ) required to reach the percolation threshold is now determined by a “double percolation effect.” Double percolation results from the dependence of electrical conductivity on both the connectivity of carbon black within a given polymer and the connectivity of that polymer within the blend. Breuer et al.<sup>23</sup> have recently been able to achieve percolation thresholds as low as 0.5 vol % carbon black using a high-impact polystyrene/linear low-density polyethylene blend. Maximum conductivity in this system appears to be on the order of  $10^{-3}$  S/cm.

Various other techniques have been used with binary composite systems to achieve significant

percolation threshold reductions, such as decreasing the level of interaction between polymer and filler through surface energy adjustment and functionality modification.<sup>2,24,25</sup> Further reductions in the percolation threshold can be achieved by changing the shape of the conductive filler and modifying the microstructure of the matrix polymer. Changing the shape of graphite filler from spheres to rods will reduce the percolation threshold, although preferential alignment of the rods tends to create anisotropic conductivity.<sup>26</sup> Polymers with a semicrystalline microstructure will also lower the percolation threshold, in a manner similar to that of a two-polymer blend. Studies using polypropylene (PP) as the matrix polymer have yielded thresholds from 2 to 5 vol % carbon black.<sup>21,24</sup> The crystalline regions of the polymer act like a second phase in which the carbon black cannot reside.<sup>27</sup> Shifting of the percolation threshold to a lower critical volume fraction of filler is the net result of the crystallinity.

Low percolation thresholds have been achieved with binary systems when the polymer matrix is formed from particles that are large relative to the size of the conductive filler.<sup>28–31</sup> Malliaris and Turner<sup>28</sup> compressed a mixture of silver powder and epoxy pellets at room temperature to create a composite with a percolation threshold of 6 vol % silver. When compacted at elevated temperature, this same composite system yielded a threshold of 35 vol % silver as a result of liquefaction of the polymer pellets and subsequent infiltration by the filler to create a random system.<sup>32</sup> At room temperature the epoxy remains solid and forces the metallic filler to occupy the surface and interstices of the polymer particles, thereby reducing the concentration required to bring about long-range conductive pathways within the composite. Malliaris and Turner<sup>28</sup> developed a model to predict the onset of percolation based on the ratio of polymer to filler particle size:

$$V_A = 50P_c[1 + (\phi/4)(R_p/R_m)]^{-1} \quad (2)$$

where  $V_A$  is the volume concentration filler characteristic of the onset of electrical conductivity,  $P_c$  is the first nonzero probability for infinitely long sequences of adjacent lattice sites occupied by conductive elements (e.g.,  $P_c = 1/3$  for a hexagonal array),  $\phi$  is a factor that depends on packing of conductive particles,  $R_p$  is the radius of the polymer particle, and  $R_m$  is the radius of the metallic particle. This rela-

tionship and experimental results show that as the ratio of polymer to metallic particle size increases, the concentration of filler required to create infinitely long conductive pathways decreases. Das et al.<sup>31</sup> took this idea to the extreme using ultrafine copper particles deposited chemically on PVC powder to achieve a percolation threshold of 0.5 vol % metal.

Extremely low percolation thresholds have also been achieved in polymer composites in which intrinsically conductive polymers (ICPs) were used as the conductive filler. Kryszewski<sup>33</sup> divided these fully organic heterogeneous conducting systems into four distinct categories: (1) mixtures of conducting crystals with inert polymer<sup>34,35</sup>; (2) conductive lattices mixed with a film-forming polymer<sup>36,37</sup>; (3) blends of processable ICPs (e.g., polyalkylthiophenes) with an inert polymer<sup>38,39</sup>; and (4) reticulate doped polymers.<sup>40,41</sup> Reticulate doped polymers are created by the addition of conductive organic molecules to a polymer matrix followed by subsequent heating to induce a microcrystalline conductive network throughout the film. Jeszka and coworkers<sup>40</sup> achieved percolation thresholds below 1 vol % filler with a 1 : 1 molar ratio of tetrathiotetracene and tetracyanoquinodimethane heated to 115°C. Banerjee et al.<sup>42</sup> obtained percolation thresholds as low as 0.0214 vol % when polyaniline particles doped with HCl were dispersed in poly(methyl methacrylate). The maximum achievable conductivity for these types of systems appears to be 0.1–1 S/cm.

Presently, composites prepared from mixtures of polymer particles [i.e., poly(vinyl acetate) (PVAc) latex and water-dispersible powder] and carbon black (CB) have been studied and compared to a composite prepared from a dispersion of CB in an aqueous solution of poly(*N*-vinylpyrrolidone) (PNVP). Initial results have shown a dramatic decrease in the percolation threshold when a particulate polymer was substituted for solution polymer as the precursor to the composite matrix.<sup>43</sup> The effect of polymer microstructure on the percolation threshold and maximum achievable conductivity is investigated here. The percolation threshold is shown to decrease from around 15 vol % to less than 2.5 vol % carbon black when PVAc latex is substituted for PNVP solution as the composite matrix starting material. Current models are employed to evaluate the experimental data and to account for microstructure-induced changes.

## EXPERIMENTAL

Three types of commercial polymers were used as composite matrices in this study. Air Products (Allentown, PA) supplied a 49.77 vol % solids in water PVAc polydisperse latex (Vinac XX210) with a glass-transition temperature ( $T_g$ ) of 34°C. Water-dispersible powder (Vinnapas RP 251), comprised of PVAc stabilized by PVA, was supplied by Wacker Polymer Systems (Adrian, MI). When cast as a film from water and dried in a vacuum dessicator, this system was found to have a  $T_g$  of 32°C. Finally, PNVP powder was purchased from Aldrich Chemicals (Milwaukee, WI) and had a molecular weight ( $M_w$ ) of 55,000 g/mol and  $T_g$  of 175°C. All of the polymers were made into aqueous suspensions or solutions with 10 vol % solids prior to composite preparation. The carbon black (Conductex 975 Ultra) used in this study was supplied by Columbian Chemicals (Atlanta, GA). Conductex CB has a 21-nm primary particle size, 1.89 g/mL density, and an  $N_2$  surface area of 242 m<sup>2</sup>/g.

Polymer suspensions and solutions containing different loadings of CB were prepared with a high-speed impeller. To begin, the amount of CB needed to create the highest loading was added to a given polymer suspension or solution at a stirring rate of 880 rpm. CB was added slowly, over a span of 5 min. During carbon black addition, 5–10 drops of DrewPlus L-483 foam-control agent (Ashland, Lexington, KY) was added to the mixture in an effort to reduce the incorporation of air. Once all of the CB had been added, the impeller rate was increased to 3600 rpm for 15 min. Successively smaller loadings were prepared by further diluting this composite mixture with more polymer suspension or solution. Composite films were created by pouring the composite mixtures into 1-in.<sup>2</sup> molds and drying for 24 h at ambient temperature and atmosphere followed by another 24-h period within a vacuum dessicator to remove residual water. The resulting composite films were 200–400 μm thick.

Composite films were removed from their molds prior to electrical conductivity measurement. The conductivity measurements were made with a Veeco FPP-5000 four-point probe apparatus (Veeco Instruments, Plainview, NY). Electrical conductivity below 10<sup>-5</sup> S/cm could not be detected with this device.

Neat polymer microstructure was evaluated prior to film formation using a cryogenic fixture mounted to a JEOL 840 scanning electron micro-

scope (SEM; JEOL USA, Peabody, MA). Liquid samples were initially frozen in liquid ethane and transferred to the cryogenic chamber where frost was sublimed. These frozen samples were then fractured and coated with platinum *in situ*. All of the dried neat polymer films were imaged using a Nanoscope III multimode scanning probe microscope (SPM; Digital Instruments, Santa Barbara, CA) operated in tapping mode (TM). Dried composite films were imaged with Hitachi S-800 and S-900 field-emission gun scanning electron microscopes (FEGSEM; Nissei Sangyo, America, Ltd., Rolling Meadow, IL), along with TM scanning probe microscopy (also known as atomic force microscopy or AFM). Films were coated with 50 Å of platinum prior to FEGSEM imaging.

## RESULTS AND DISCUSSION

### Polymer Matrix Microstructure

Microstructure is the key difference between these three polymer starting materials (Fig. 1), all of which have similar surface energies and utilize water as their solvent. In Figure 1(a), a cryo-SEM image of the latex reveals a polydisperse agglomeration of spheres suspended in ice. These polymeric spheres are stabilized by PVA and have a number-average particle size of 108 nm [Fig. 2(a)] and volume-average particle size of 2.5  $\mu\text{m}$  [Fig. 2(b)] with a broad particle size distribution brought about during the semicontinuous polymerization process used to create them. The second microstructure, shown in Figure 1(b), is a water-dispersible powder stabilized by hydrophilic PVA that has been incorporated into the polymer particles. The powder has a higher level of polydispersity than does the latex, based on the volume percentage particle size analysis, with a mean particle size of 27.5  $\mu\text{m}$  [Fig. 2(b)], but has nearly the same approximate number-average particle size of 105 nm [Fig. 2(a)]. In both the powder and latex, the polymeric material is dispersed, not dissolved like the PNVP solution shown in Figure 1(c). Here, the polymer chains are completely dissolved in water and there is no apparent microstructure. The formation of ice microcrystals during the freezing process that precedes cryoimaging gives the PNVP fracture surface some texture that would not be present at room temperature.

Despite being more polydisperse, tapping-mode atomic force microscope (TMAFM) images

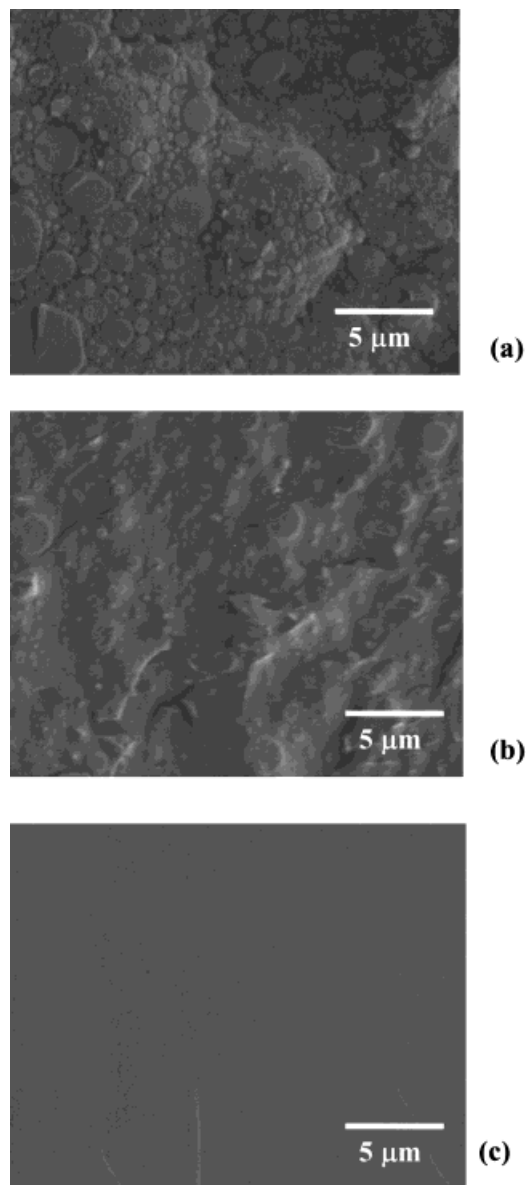


**Figure 1** Cryo-SEM images of three polymer microstructures: polydisperse PVAc latex (a), polydisperse PVAc water-dispersible powder (b), and PVP dissolved in water.

of the surface of the dried neat polymer films make the PVAc powder appear to have a similar particle size distribution to that of the PVAc latex (Fig. 3). During the drying process the largest PVAc powder particles settle out of the dispersion, leaving smaller particles with a narrower distribution at the film surface. Particle size analysis performed after the latex and powder dispersions had been allowed to settle for 24 h (Fig. 4), show that the largest particles settle out of the powder dispersion but remain suspended in the

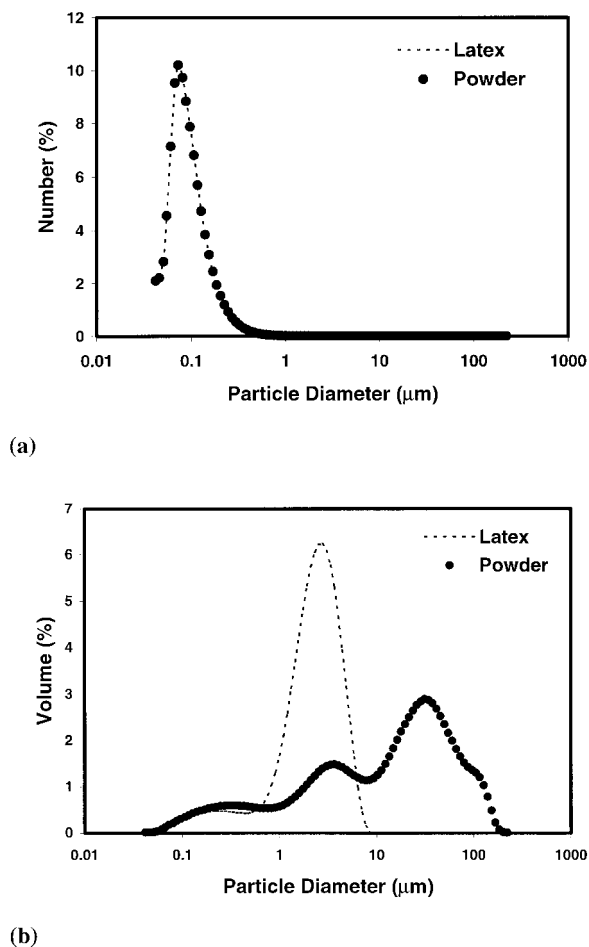


**Figure 2** Number percentage (a) and volume percentage (b) particle size analysis of PVAc latex (—), and water-dispersible powder (●).

latex. Samples for particle size analysis were qualitatively taken from the bottom, middle, and top of a 60-mL vial. In Figure 4(a), the particle size distribution grows narrower, with a smaller mean particle size, because the samples are taken closer to the top of the vial for the PVAc powder. The mean particle size and shape of particle size distribution stays essentially the same for the latex at all locations within the sample vial [Fig. 4(b)].

In Figure 3, both height [Fig. 3(a)] and amplitude [Fig. 3(b)] images of the surface of the neat PVAc latex film are shown to illustrate the differences between images captured in each of the two modes. Film topography is reflected in the height image, whereas fine features are better revealed in the amplitude image.<sup>44</sup> Deflection of the cantilever against the sample surface damps the am-

plitude of cantilever oscillation. The AFM adjusts to a constant level of oscillation and thereby keeps the tip a constant distance from the sample surface. The amplitude signal is fed through a feedback circuit, which converts the data to height information. The feedback circuit actually departs from a prescribed constant amplitude value in a manner akin to the first derivative of the topography. Amplitude images are often referred to as the error signal as a result of the preceding observations. Local changes in slope give the amplitude image the impression of being illuminated from the side. In the case of the PVP film [Fig. 3(d)], the smooth, nearly featureless surface shows some subtle texture using the amplitude image but would show nothing in a height image. All subsequent AFM images will be amplitude images as a result of their enhanced resolution of subtle surface features.

Another observation that can be made from Figure 3 is that it appears that the PVAc powder is better coalesced than is the PVAc latex. Figure 3(d) may be especially deceiving when evaluating the level of coalescence of the PVAc powder. Neither type of film is completely coalesced but the latex is visually transparent and experimentally measured  $T_g$  and elastic modulus match values quoted by the manufacturer, suggesting that, from a practical standpoint, the films are sufficiently coalesced. Dried films made from the PVAc powder are opaque with a yellowish hue resulting from additives incorporated by the manufacturer. Furthermore, the powder films have a large scatter in modulus and  $T_g$  data that suggest incomplete practical coalescence. This water-dispersible powder is used in the manufacture of gypsum wall troweling compounds, joint fillers, and/or wood adhesive. It contains no film-forming agents and was not developed to act as a stand-alone film.<sup>45</sup> Poly(vinyl alcohol) (PVA) is used to stabilize the powder when it is redispersed into water. The PVA likely dissociates somewhat from the PVAc particles as it is solvated in the water and is then deposited at the top of the film during drying. This PVA layer obscures the true state of the particles in the dried film. Examining cross sections of the two types of films provides a more accurate depiction of film coalescence. Figure 5 shows freeze-fractured cross sections of dried latex and powder films. From these images it becomes clear that the latex is coalesced the same as or better than the powder film.

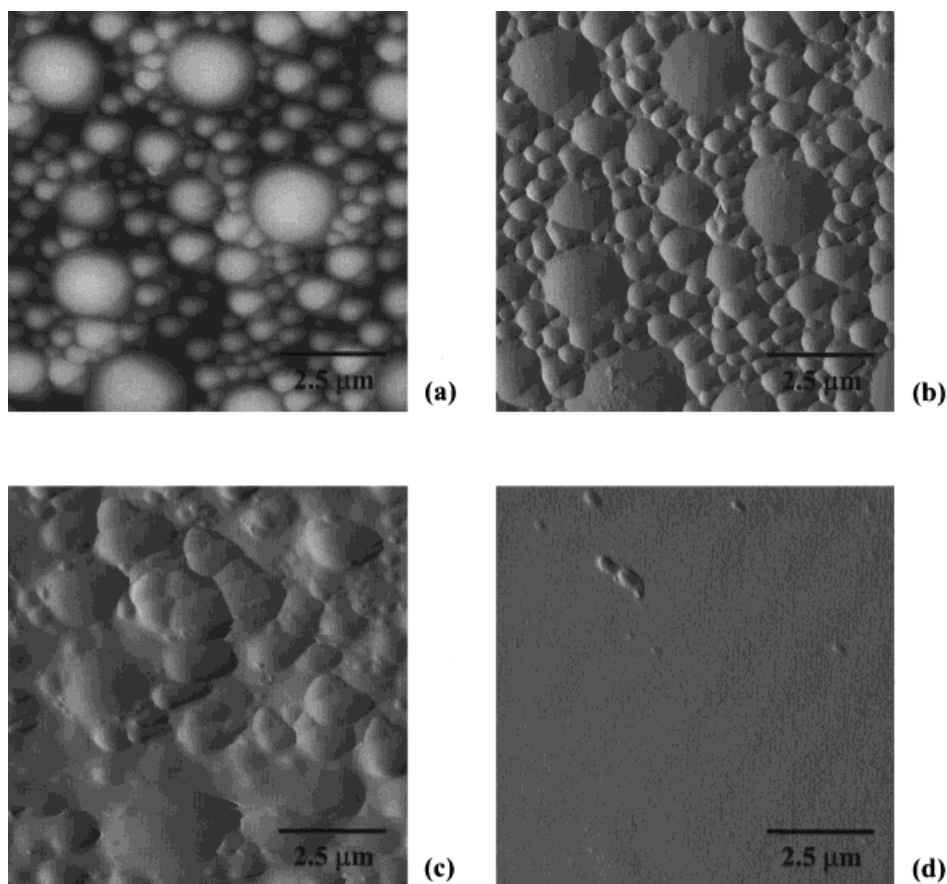


**Figure 3** TMAFM images of dried, neat polymer films: height (a) and amplitude (b) of PVAc latex, amplitude of PVAc powder (c), and amplitude of PVP (d).

### Composite Microstructure

Once the conductive filler (e.g., carbon black) has been added to a given polymer microstructure, the differences in CB distribution between the solution and suspension (or particulate) systems become quite striking. Figure 6 shows TMAFM free surface images of the three systems under consideration at carbon black concentrations of 4, 9, and 15 vol %. The two polymer suspension-based systems (i.e., water-dispersible powder and latex) create a segregated network of carbon black particles, even at very low concentrations of filler. For composites cast using the solution-based PNVP, the CB particles appear more randomly distributed. The relatively large depressions seen in the powder image loaded with 15 vol % carbon black [Fig. 6(f)] are actually a consequence of porosity that results at high filler loading. These pores can alter the predicted electrical conductivity, as will be shown.

Increased carbon black concentration within a composite does not necessarily manifest itself in

the surface images shown in Figure 6, but is very apparent in images taken through the bulk (Fig. 7). Fractured cross sections of the three composite systems loaded with 9 and 15 vol % carbon black show that segregation occurs throughout the thickness for the latex [Fig. 7(a) and (b)] and water-dispersible powder systems [Fig. 7(c) and (d)]. More random placement of filler characterizes the PNVP matrix composite [Fig. 7(e) and (f)]. Carbon black particles appear as white dots in these images because of their small size, creating sharp features that readily emit secondary electrons. An intricate charging pattern can also be observed in the PNVP solution-based composite resulting from the lack of sufficient electrical conductivity. The two suspension-based systems are actually quite conductive when filled with 9 vol % carbon black and therefore exhibit no charging. Some minor porosity is observed for the suspension-based composites that is not present in the PNVP composite system at this level of filler loading.

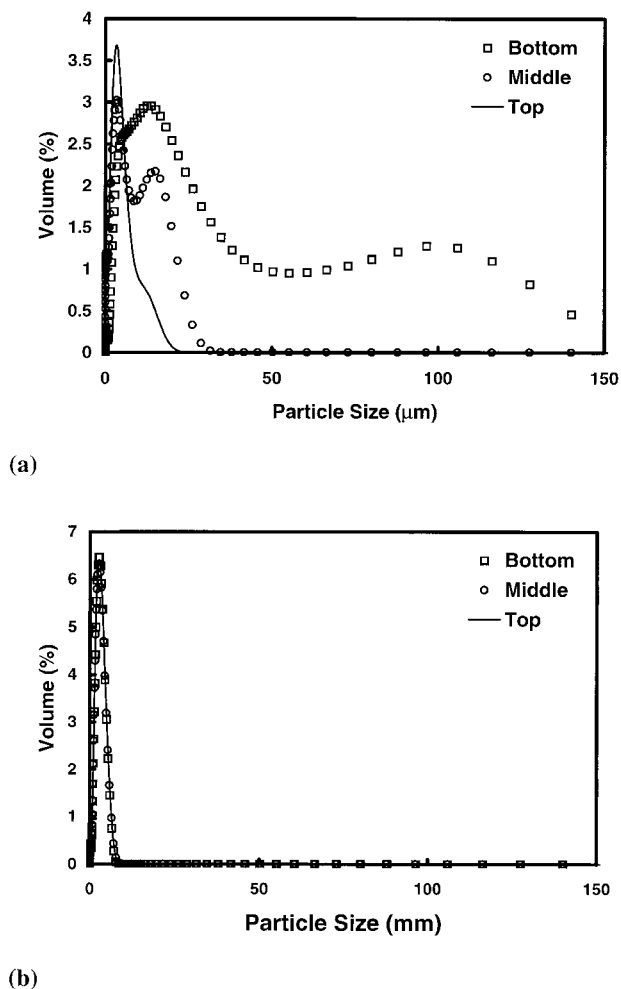


**Figure 4** Particle size analysis of bottom ( $\square$ ), middle ( $\circ$ ); top (—) of 60 mL sample vial after 24 h of settling for the PVAc water-dispersible powder (a) and latex (b).

### Composite Conductivity

The effect of CB loading on conductivity for each of three composite systems (Fig. 8) clearly shows a dramatic difference in percolation threshold between the solution-based composite system and the two suspension-based systems. The PNVP-matrix composite has a percolation threshold around 15 vol % CB and illustrates the type of random resistor system described by classical percolation theory.<sup>46</sup> As the composite mixture dries, the CB particles are free to situate themselves anywhere within the polymer matrix, as shown in Figure 6(a)–(c). When the polymer suspension-based composites are drying, however, the carbon black can situate itself only between individual polymer particles. This lack of random CB placement leads to a lowered percolation

threshold as conductive pathways are formed at lower filler concentrations. The solid curve shown in Figure 8 is the fit to the experimental data for the latex composite using the empirical percolation formula. Percolation parameters for all of the composite systems are summarized in Table I.

The most striking difference in percolation threshold is between the PNVP composite, at about 15 vol % CB, and the PVAc latex-based composite, at about 2.5 vol % CB. This near-order-of-magnitude change in carbon black concentration required to bring about macroscopic electrical conductivity appears to result from the segregation brought about by the latex particulate microstructure. The jump in electrical conductivity for these composite systems is directly linked to the formation of conductive filler pathways; therefore, CB segregation in the composites with the particulate polymer matrix would be expected to have a much lower carbon black percolation threshold than that of their solution-based counterpart. Despite having a higher percolation threshold than that of the particulate microstructures, the solution-based PNVP composite achieves a greater value of maximum conductivity at the high end of carbon black loadings studied here.

The percolation threshold ( $V_A$ ) was calculated for each of the composite systems (Table I) using the model proposed by Malliaris and Turner.<sup>28</sup> Two values of  $V_A$  were computed for each composite type, the first using the number-average polymer particle size and the second using the volume-average polymer particle size. For the PNVP-based composite, the polymer particle size was taken to be identical to that of carbon black to achieve random placement of filler. Percolation thresholds ( $V_c$ ), determined by fitting experimental values, for both of the suspension-based composites fall between the two calculated  $V_A$  values. The use of number-average particle size results in a  $V_A$  much closer to experiment. This result is somewhat intuitive because a small fraction of large particles dramatically increases the volume-average polymer particle size without contributing significantly to the true physical situation. In all cases the carbon black particles were assumed to be packed in a hexagonal arrangement (i.e., having a coordination number of 6), causing the values of  $\phi$  and  $P_c$  in eq. (2) to be 1.11 and 0.33, respectively. According to the assumptions made by Malliaris and Turner, the composites prepared with the water-dispersible PVAc powder should have a similar or smaller  $V_A$  than

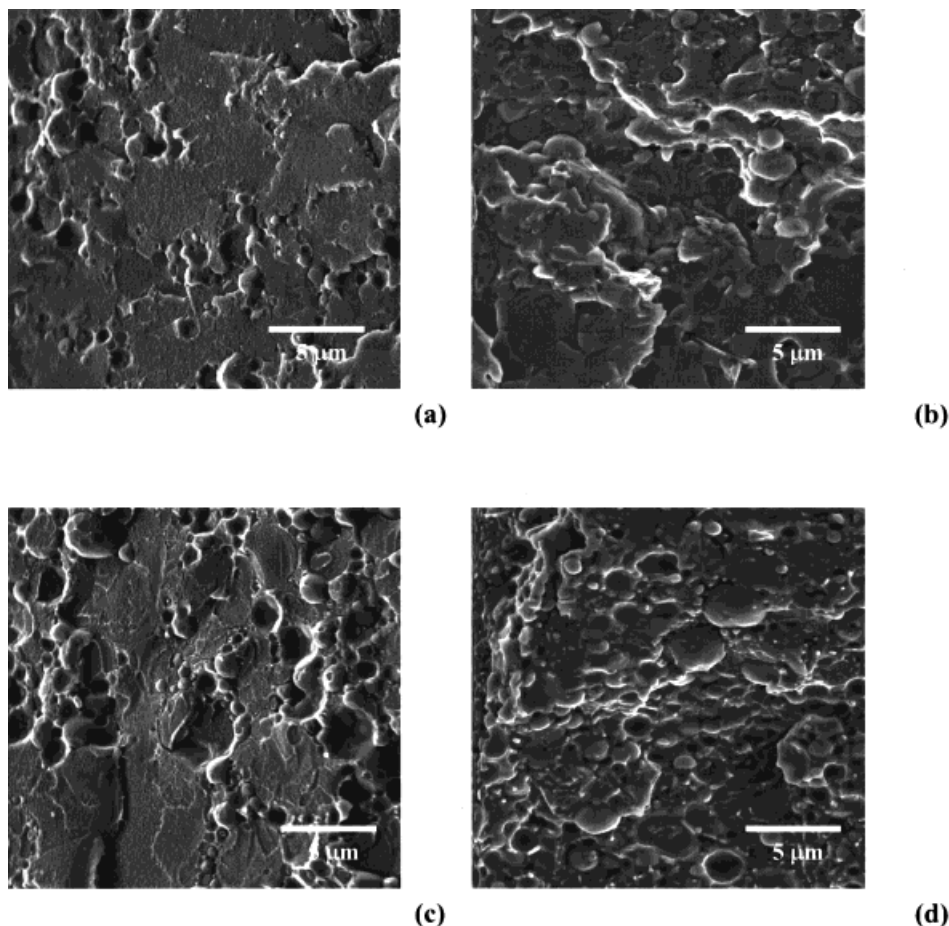


**Figure 5** FEGSEM images of PVAc latex, taken from the top (a) and bottom (b) of a cross section, and water-dispersible powder, taken from the top (c) and bottom (d) of a cross section.

that made with the PVAc latex because of similar number-average particle size and much larger volume-average particle size. Some of the discrepancy between theory and experiment may be accounted for by the settling of PVAc powder particles that occurs during composite drying. Another source of disparity lies in the arrangement of carbon black around the polymer particles. Malliaris and Turner assumed that a monolayer of conductive particles existed around each polymer particle, which is certainly not the case experimentally, as seen in Figure 6. Finally, the high level of polydispersity in both suspension systems is certainly a source of error when making comparisons to the model of Malliaris and Turner, who were targeting systems that are much more monodisperse. On a qualitative level, the agreement between experiment and theory is actually quite good.

It is interesting to note the small values of the critical exponent ( $s$ ) obtained when fitting the per-

colation power law for the two particulate-based composite systems. Data shown in Table I were calculated using a weighted, linear regression method applied to the entire data set. It should be noted that the critical exponent can change significantly (e.g., 20%) depending on the fitting procedure, whereas the percolation threshold is much less sensitive. For three-dimensional random resistors,  $s$  is typically between 1.6 and 2.<sup>47</sup> Higher values of  $s$  are exhibited by other segregated CB-polymer systems in which a reduced percolation threshold has been seen.<sup>21,24,27,48</sup> For example, Foulger<sup>47</sup> obtained reduced percolation thresholds when using a semicrystalline polymer (i.e., HDPE) as the composite matrix in conjunction with carbon black, although the value of  $s$  was close to 3. He suggested that an exponent greater than 2 was the result of additional conduction mechanisms or a “percolation-within-percolation” phenomenon. Heaney<sup>49</sup> found that mean-field theory was able to adequately describe these



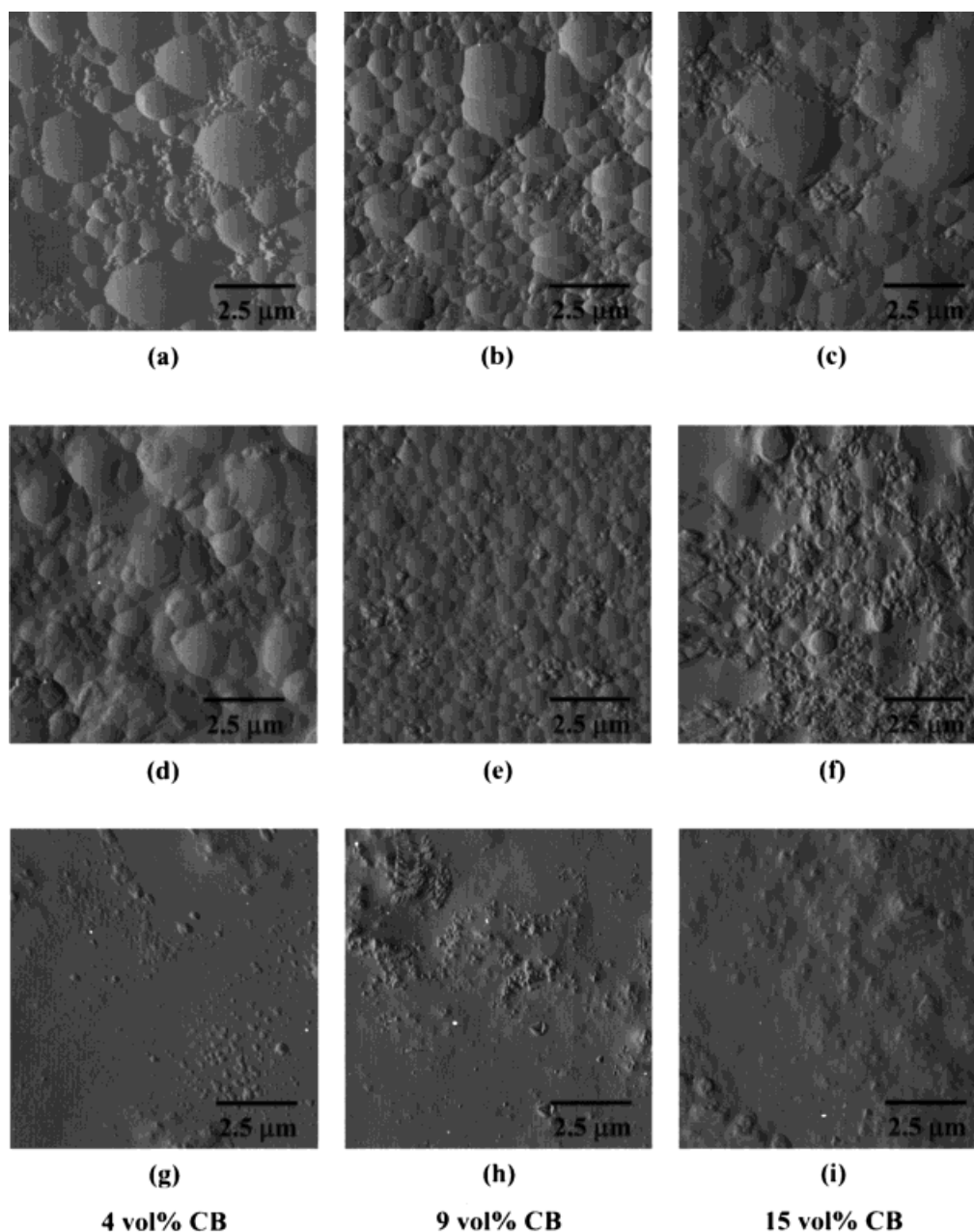


**Figure 6** TMAFM images of the PVAc latex (a–c), PVAc water-dispersible powder (d–f), and PVP (g–i) composites filled with 4, 9, and 15 vol % carbon black, respectively, from left to right.

“nonuniversal” systems. Furthermore, he goes on to suggest that exponents much greater than 2 are seen in systems obeying continuum percolation, whereas those with values in the universal range of 1.6–2 obey some type of matrix percolation. On the lower end of this range, the organization of the percolation network may occur in a more ordered fashion.

Slupkowski<sup>50</sup> developed a model to describe segregated composite systems that allows electri-

cal conductivity to be predicted at any filler concentration beyond the percolation threshold ( $V_c$ ). This model was developed for a dry mixture of conducting and insulating particles in which the diameter of insulating particles is assumed to be much larger than that of the conductive particles. The insulating particles are thought to form a connected cubic network with a uniform coating of conductive particles. These assumptions result in the following relationship:

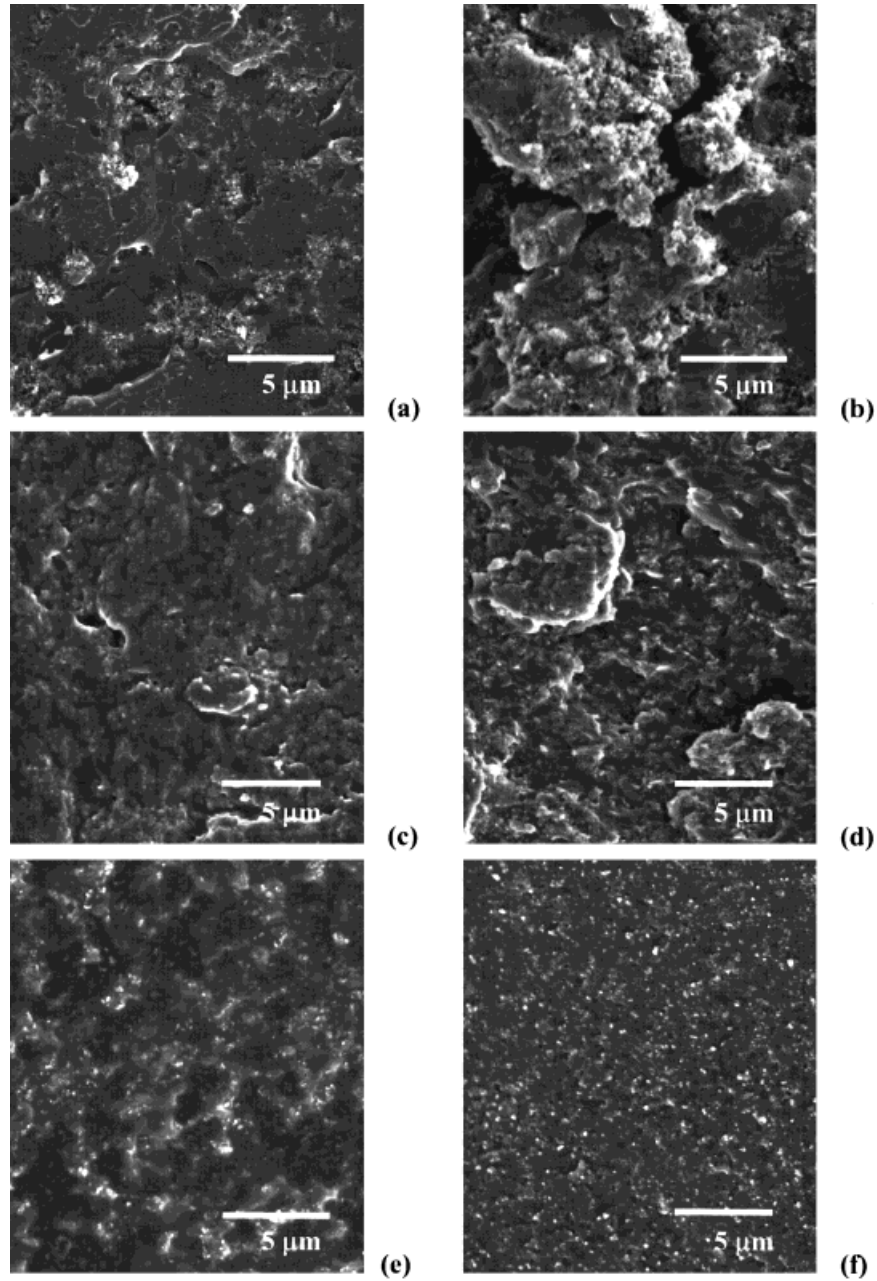


**Figure 7** FEGSEM freeze-fractured cross sections of PVAc latex (a, b), PVAc water-dispersible powder (c, d), and PNVP (e, f) all filled with 9 and 15 vol % CB, respectively.

$$\sigma = 2\pi\sigma_c \frac{d([x] + P)}{D \ln\left(1 + \frac{D}{([x] + 1)d}\right)} \quad (3)$$

$$[x] = \left( \sqrt[3]{\frac{1}{1-V}} - 1 \right) \frac{D}{2d} \quad (4)$$

where  $\sigma$  is the resulting composite conductivity,  $\sigma_c$  is the intrinsic conductivity of the filler (taken to be 7 S/cm for carbon black),  $d$  is the conductive particle diameter,  $D$  is the insulating particle diameter,  $[x]$  is the number of totally filled sublayers of thickness  $d$  and is defined by:

and  $P$  is the probability for the occurrence of a conductive network consistent with a percolation threshold and was obtained using the model by Scarsbrick<sup>51</sup>:

$$P = V^{V-2/3} \quad (5)$$

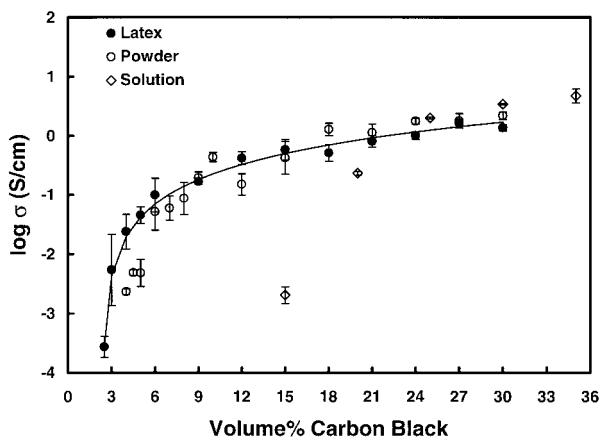


**Figure 8** Log conductivity versus vol % carbon black for the three composite systems under examination: PVAc latex (●), PVP solution (◇), and PVAc water-dispersible powder (○). The empirically determined classical percolation curve [based on eq. (1)] has been included for the PVAc latex (—) using the parameters listed in Table I.

where  $V$  is the volume fraction of conductive filler.  $D$  was taken to be the number-average particle size for the two systems obtained from particle size analysis previously discussed.

A comparison of Slupkowski's model with the experimental data for the water-dispersible powder and latex composites is shown in Figure 9. The model appears to qualitatively agree with experimental data at low carbon black concentrations but diverges at loadings above 20 vol %. This discrepancy at high carbon black concentration most likely results from the formation of porosity in the composites (Fig. 10) that is not accounted for in this model. Porosity arises in these composites as a result of the inability of the polymer matrix to sufficiently envelop the filler particles, resulting in small interstitial voids that grow as the filler concentration is further increased. At high filler concentrations this porosity appears to become networked

and tends to cause composite electrical conductivity to level off faster than theory would predict as a result of breakup of conductive pathways.<sup>52</sup> This discrepancy is consistent with a pore percolation threshold for mechanical behavior occurring at the critical pigment volume concentration (CPVC), which will be reported in a future publication.<sup>53</sup> Composites with such high CB loadings would not be prepared in practice.

Slupkowski's model also predicts percolation thresholds well below those found experimentally. In Figure 9, the Slupkowski model shows a significant level of electrical conductivity ( $>10^{-4}$  S/cm), even at 1 vol % carbon black, whereas conductivity dropped below  $10^{-5}$  S/cm below 2.5 vol % carbon black experimentally. The composite matrices were created using very polydisperse polymer microstructures, thereby eliminating the possibility of a regular cubic network of insulating particles as Slupkowski assumes. Another deviation from Slupkowski's idealized model comes from the nonuniformity of the carbon black coating on the polymer particles (Fig. 6). The next logical step would be to create composites using a nearly monodisperse latex and comparing the resulting percolation threshold and conductivity as a function of CB concentration to that predicted by Malliaris and Turner, and Slupkowski.

## CONCLUSIONS

The percolation threshold of carbon black-filled polymer composites can be dramatically reduced when a suspension-type polymer system is used to form the composite matrix. A PNVP-CB composite was found to have a percolation threshold near 15 vol % carbon black, although this value diminished to less than 3 vol % CB when PNVP was replaced by a PVAc latex. In addition to providing a lower percolation threshold, conductive

**Table I** Percolation Parameters and Percolation Threshold Predictions

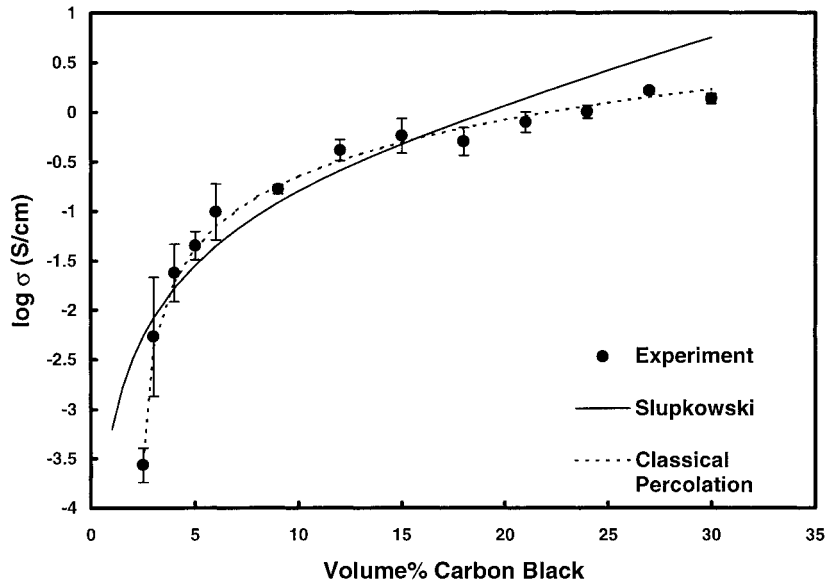
Matrix	$\sigma_0$ (S/cm)	$100V_c^a$	$s$	$R^2$	$V_A^b$	$V_A^c$
Latex	$12.8 \pm 1.8$	$2.39 \pm 0.04$	$1.57 \pm 0.08$	0.99	6.87	0.49
Powder	$35.1 \pm 6.6$	$3.44 \pm 0.11$	$1.88 \pm 0.09$	0.99	6.98	0.05
Solution	$251.9 \pm 42.3$	$14.5 \pm 0.04$	$2.25 \pm 0.09$	0.94	$13.05^d$	$13.05^d$

<sup>a</sup> This is the percolation threshold determined empirically using eq. (1).

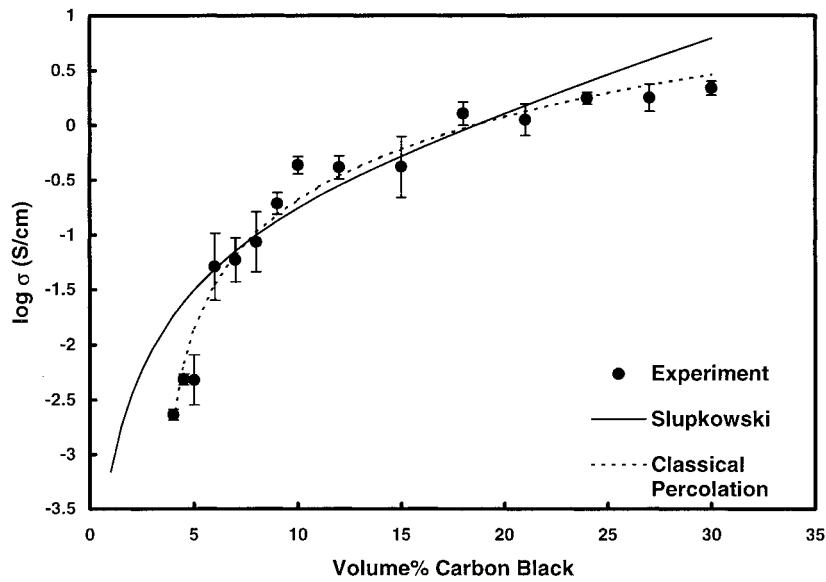
<sup>b</sup> Calculated from eq. (2) based on number average value for polymer particle size.

<sup>c</sup> Calculated from eq. (2) based on volume average value for polymer particle size.

<sup>d</sup> Both number and volume particle size taken to be equal to that of the carbon black particle, 21 nm.



(a)



(b)

**Figure 9** Comparison of Slupkowski's model (—) with classical percolation theory (---) and experimental conductivity data (●) for the PVAc latex (a) and the water-dispersible powder (b).

composites prepared with a dispersed particle matrix starting material can be created without the use of pressure, heat, or dopants that are required for similar results in other systems. The latex-carbon black system studied here has an excellent combination of low percolation threshold and high maximum achievable conductivity

( $\sigma_{max}$ ), compared with that of other polymer composite systems described in the literature. The particulate microstructure of the latex effectively forces carbon black into conductive pathways during drying, so that percolation occurs at much lower filler concentrations. Theoretical models dealing with segregated composite microstruc-

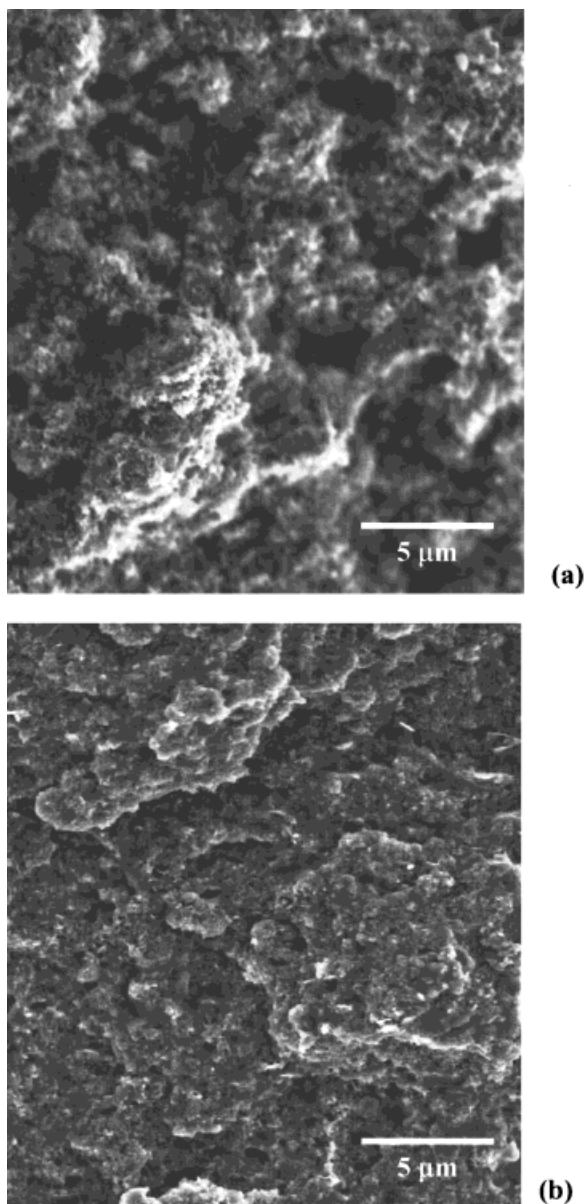


**Figure 10** FEGSEM images of PVAc latex (a), PVAc water-dispersible powder (b), and PVP filled with 18 vol % CB.

tures similar to the latex-based system qualitatively predict electrical conductivity and the location of the percolation threshold. The particulate polymer microstructures examined here were very polydisperse and, therefore, difficult to correlate to models based on monodisperse systems. Future studies of segregated composites, which incorporate monodisperse polymer microstructures, will lead to a more fundamental understanding of the observed behavior.

The authors acknowledge support from Eastman Kodak Co. and the Industrial Partnership for Research in Interfacial and Materials Engineering (IPRIME), through its Coating Process Fundamentals Program. The authors also thank Dr. Ashok Menon for cryo-SEM imaging, Melissa Grunlan for particle size analysis, and Dr. Michael Heaney for thoughtful discussion.

## REFERENCES

1. Bigg, D. M.; Stutz, D. E. *Polym Comp* 1983, 4, 40.
2. Reboul, J. P. in *Carbon Black-Polymer Composites*; Sichel, K., Ed.; Marcel Dekker: New York, 1982, Chapter 3.
3. Sau, K. P.; Chaki, T. K.; Chakraborty, A.; Khastgir, D. *Plast Rubber Compos Process Appl* 1997, 26, 291.
4. Lundberg, B.; Sundqvist, B. *J Appl Phys* 1986, 60, 1074.
5. Lewis, N. S.; Lonergan, M. C.; Severin, E. J.; Doleman, B. J.; Grubbs, R. H. *SPIE* 1996, 3079, 660.
6. Ruschau, G. R.; Newnham, R. E.; Runt, J.; Smith, B. E. *Sens. Actuators* 1989, 20, 269.
7. Talik, P.; Zabkowska-Waclawek, M.; Waclawek, W. *J Mater Sci* 1992, 27, 6807.
8. Moffat, D. M.; Runt, J. P.; Halliyal, A.; Newnham, R. E. *J Mater Sci* 1989, 24, 609.
9. Yi, X. S.; Wu, G.; Ma, D. *J Appl Polym Sci* 1998, 67, 131.
10. Leclere, Ph.; Lazzaroni, R.; Gubbels, F.; Calberg, Ph.; Dubois, C.; Jerome, R.; Bredas, J. L. *Mater Res Soc Symp Proc* 1997, 457, 475.
11. Stauffer, D. *Phys Rep* 1979, 54, 1.
12. Donnet, J. B.; Bansal, R.; Wang, M. in *Carbon Black Science and Technology*; Marcel Dekker: New York, 1993, Chapter 8.
13. Carmona, F. *Physica A* 1989, 157, 461.
14. Zhang, M. Q.; Yu, G.; Zeng, H. M.; Zhang, H. B.; Hou, Y. H. *Macromolecules* 1998, 31, 6724.
15. Sumita, M.; Abe, H.; Kayaki, H.; Miyasaka, K. *J Macromol Sci Phys B* 1986, 25, 171.
16. Tang, H.; Chen, X.; Tang, A.; Luo, Y. *J Appl Polym Sci* 1996, 59, 383.
17. Scher, H.; Zallen, R. *J Chem Phys* 1970, 53, 3759.
18. Kirkpatrick, S. *Rev Mod Phys* 1973, 45, 574.
19. Medalia, A. I. *Rubber Chem Technol* 1986, 59, 432.
20. Sumita, M.; Sakata, K.; Asai, S.; Miyasaka, K.; Nakagawa, H. *Polym Bull* 1991, 114, 4917.
21. Tchoudakov, R.; Breuer, O.; Narkis, M. *Polym Eng Sci* 1996, 36, 1336.
22. Feng, J.; Chan, C.-M. *Polym Eng Sci* 1998, 38, 1649.
23. Reboul, J. P. in *Carbon Black-Polymer Composites*; Sichel, K., Ed.; Marcel Dekker: New York, 1982, Chapter 1.
24. Miyasaka, K.; Watanabe, K.; Jojima, E.; Aida, H.; Sumita, M.; Ishikawa, K. *J Mater Sci* 1982, 17, 1610.

25. Nielsen, L. E. *Ind Eng Chem Fundam* 1974, 13, 17.
26. Balta Calleja, F. J.; Bayer, R. K.; Ezquerro, T. A. *J Mater Sci* 1988, 23, 1411.
27. Zhang, M.; Jia, W.; Chen, X. *J Appl Polym Sci* 1996, 62, 743.
28. Malliaris, A.; Turner, D. T. *J Appl Phys* 1971, 42, 614.
29. Battacharya, S. K.; Basu, S.; De, S. K. *Composites* 1978, 9, 117.
30. Rajagopal, C.; Satyam, M. *J Appl Phys* 1978, 49, 5536.
31. Das, D.; Basu, S.; Paul, A. *J Mater Sci* 1980, 15, 1719.
32. Gurland, J. *Trans Met Soc AIME* 1966, 236, 642.
33. Kryszewski, M. *Synth Met* 1991, 45, 289.
34. Ikeno, S.; Yokoyama, M.; Mikawa, H. *Polym J* 1977, 10, 123.
35. Kita, H.; Okamoto, K.; Mukai, S. *J Appl Polym Sci* 1986, 31, 1338.
36. Cassignol, C.; Cavarero, M.; Boudet, A.; Ricard, A. *Polymer* 1999, 40, 1139.
37. Cooper, E. C.; Vincent, B. *J Phys D Appl Phys* 1989, 22, 1580.
38. Chiang, C. K. *Polymer* 1981, 22, 1454.
39. Ingans, O. *Br Polym J* 1988, 20, 333.
40. Jeszka, J. K.; Ulanski, J.; Kryszewski, M. *Nature (London)* 1981, 289, 390.
41. Tracz, A.; Kryszewski, M. *Macromol Chem* 1989, 15, 219.
42. Banerjee, P.; Mandal, B. M. *Macromolecules* 1995, 28, 3940.
43. Grunlan, J. C.; Gerberich, W. W.; Francis, L. F. *Mater Res Soc Symp Proc* 1999, 525, 475.
44. Magonov, S. *Digital Instruments Application Notes*, 1998.
45. Vinnapas<sup>®</sup> RP 251 Technical Data Sheet; Wacker Polymer Systems, 1999.
46. Stauffer, D.; Aharony, A. *Introduction to Percolation Theory*, 2nd ed.; Taylor & Francis: London, 1992, Chapter 5.
47. Deutscher, G.; Kapitulnik, A.; Rappaport, M. in *Percolation Structures and Processes*; Deutscher, G.; Zallen, R.; Adler, J., Eds.; *Annals of the Israel Physical Society*, Vol. 5; American Institute of Physics: New York, 1983, Chapter 10.
48. Foulger, S. H. *J Appl Polym Sci* 1999, 72, 1573.
49. Heaney, M. B. *Phys Rev B* 1995, 52, 12477.
50. Slupkowski, T. *Phys Status Solidi A* 1984, 83, 329.
51. Scarsbrick, R. M. *J Phys D Appl Phys* 1973, 6, 2098.
52. Grunlan, J. C.; Gerberich, W. W.; Francis, L. F. *J Mater Res* 1999, 14, 4132.
53. Grunlan, J. C.; Francis, L. F.; Gerberich, W. W. Unpublished results, 1999.